Molecular Plant Pathology

MOLECULAR PLANT PATHOLOGY DOI: 10.1111/mpp.12433

Xanthomonas citri ssp. *citri* requires the outer membrane porin OprB for maximal virulence and biofilm formation

FLORENCIA A. FICARRA[1], CAROLINA GRANDELLIS[1], ESTELA M. GALVÁN[2], LUIS IELPI[2], REGINA FEIL[3], JOHN E. LUNN[3], NATALIA GOTTIG[1] AND JORGELINA OTTADO[1,*]

[1]*Instituto de Biología Molecular y Celular de Rosario, Consejo Nacional de Investigaciones Científicas y Técnicas (IBR-CONICET) and Facultad de Ciencias Bioquímicas y Farmacéuticas, Universidad Nacional de Rosario, Ocampo y Esmeralda, Rosario 2000, Argentina*

[2]*Laboratory of Bacterial Genetics, Fundación Instituto Leloir, IIBBA-CONICET (C1405BWE), Ciudad de Buenos Aires, Buenos Aires, Argentina*

[3]*Max Planck Institute of Molecular Plant Physiology, Wissenschaftspark Potsdam-Golm, Am Mühlenberg 1, 14476 Potsdam-Golm, Germany*

SUMMARY

Xanthomonas citri ssp. *citri* (Xcc) causes canker disease in citrus, and biofilm formation is critical for the disease cycle. OprB (Outer membrane protein B) has been shown previously to be more abundant in Xcc biofilms compared with the planktonic state. In this work, we showed that the loss of OprB in an *oprB* mutant abolishes bacterial biofilm formation and adherence to the host, and also compromises virulence and efficient epiphytic survival of the bacteria. Moreover, the *oprB* mutant is impaired in bacterial stress resistance. OprB belongs to a family of carbohydrate transport proteins, and the uptake of glucose is decreased in the mutant strain, indicating that OprB transports glucose. Loss of OprB leads to increased production of xanthan exopolysaccharide, and the carbohydrate intermediates of xanthan biosynthesis are also elevated in the mutant. The xanthan produced by the mutant has a higher viscosity and, unlike wild-type xanthan, completely lacks pyruvylation. Overall, these results suggest that Xcc reprogrammes its carbon metabolism when it senses a shortage of glucose input. The participation of OprB in the process of biofilm formation and virulence, as well as in metabolic changes to redirect the carbon flux, is discussed. Our results demonstrate the importance of environmental nutrient supply and glucose uptake via OprB for Xcc virulence.

Keywords: biofilm, citrus canker, OprB, *Xanthomonas citri* ssp. citri.

INTRODUCTION

Xanthomonas citri ssp. *citri* (Xcc) is the phytopathogen responsible for citrus canker. The disease affects all citrus plants, causing significant economic losses worldwide, directly as a result of defoliation and premature fruit drop and thus yield, and also as a result of quarantine restrictions that limit the movement of fresh fruit (Graham *et al.*, 2004). Xcc enters citrus tissue through stomata or wounds and colonizes the apoplast. Translocation of effector proteins into the plant cell then takes place, and host metabolism reprogramming leads to cell hypertrophy and hyperplasia, which results in the typical raised corky cankers in fruits, leaves and stems (Brunings and Gabriel, 2003).

Xcc forms biofilm structures to complete the disease cycle (Gottig *et al.*, 2010; Zimaro *et al.*, 2013) and many proteins are involved in this process. Previously, in a comparative proteomic study carried out on Xcc mature biofilm and planktonic cells, major variations in the composition of outer membrane proteins and receptor or transport proteins were revealed. Among the differentially expressed proteins in biofilms compared with the planktonic cells, several porins and TonB-dependent receptor proteins were identified, suggesting that these proteins have specific membrane-associated functions, including signalling and cellular homeostasis (Zimaro *et al.*, 2013). One of the proteins found to be up-regulated in Xcc biofilms was OprB (Outer membrane protein B), a 41.3-kDa protein which is 31% identical and 48% similar to *Pseudomonas aeruginosa* OprB protein. This protein is encoded by XAC2504 and was previously named RpfN (Moreira *et al.*, 2004, 2010; Zimaro *et al.*, 2013, 2014), as a protein belonging to the *rpf* (*regulator of pathogenicity factors*) regulon. In *Xanthomonas campestris* pv. *campestris*, the *rpf* gene cluster contains genes from *rpfA* to *rpfI* and is responsible for the synthesis, detection and signal transduction of DSF (Diffusible Signal Factor) which mediates quorum sensing (Tang *et al.*, 1991). RpfC and RpfG are the histidine kinase and its associated response regulator, respectively, in the two-component regulatory system. This system regulates the expression of the genes that code for RpfB and RpfF, a long-chain fatty acid-coenzyme A (CoA) ligase and an enoyl-CoA hydratase, respectively, and are involved in the synthesis of DSF (Barber *et al.*, 1997; Slater *et al.*, 2000). Further, the *rpf* cluster also regulates virulence activities, such as the production of extracellular enzymes and the extracellular polysaccharide (EPS) xanthan (Barber *et al.*, 1997; Tang *et al.*, 1991; Slater *et al.*, 2000). In Xcc, the *rpf* cluster is broadly conserved, although *rpfH* and *rpfI* are absent (da Silva *et al.*, 2002). Further analyses have shown that Xcc deletion mutant strains in the three genes *rpfF*, *rpfC* and *rpfG*, involved in DSF synthesis, detection and

* *Correspondence*: Email: ottado@ibr-conicet.gov.ar

transduction, are less virulent, secrete less proteases and show decreased motility (Guo *et al.*, 2012). With regard to XAC2504, no regulation by the *rpf* regulon has been observed in either Xcc (Guo *et al.*, 2012) or *X. campestris* pv. *campestris* (An *et al.*, 2013; O'Connell *et al.*, 2013). Nevertheless, this gene was initially misnamed *rpfN* (Moreira *et al.*, 2010) citing a report in which *X. campestris* pv. *campestris rpfE* mutants were studied (Dow *et al.*, 2000). In view of this, we renamed XAC2504 as *oprB*.

OprB homologues in *Pseudomonas* spp. and *Burkholderia* spp. function in a similar manner to the specific carbohydrate porin. In *Pseudomonas putida*, OprB is induced by growth on minimal medium supplemented with glucose as the sole carbon source (Saravolac *et al.*, 1991) and repressed by succinate and other organic acids (Shrivastava *et al.*, 2011). Moreover, *P. aeruginosa* mutants lacking *oprB* are deficient in the passage of glucose across the outer membrane and also of other sugars, including mannitol, fructose and glycerol. Thus, OprB is thought to function as a porin for the transport of monosaccharides and small sugar alcohols, playing a central role in carbohydrate uptake (Wylie and Worobec, 1995). The structure of the OprB channel from *P. putida* F1 has been solved; it forms a monomeric, 16-stranded, β-barrel with seven loops and a constriction pore formed by two extracellular loops (L2 and L3). This channel constriction holds the side chains of two highly conserved arginine residues and a conserved glutamate that interact with a bound glucose molecule (van den Berg, 2012). Liposome swelling assays also showed a strong preference for OprB to transport monosaccharides over disaccharides, with glucose being a preferred substrate (van den Berg, 2012).

The genus *Xanthomonas* is characterized by the production of the EPS xanthan, which is widely used as a viscosifying, stabilizing, emulsifying or gelling agent (Sutherland, 1998). Xanthan is synthesized from sugar nucleotide precursors. It consists of repeating pentasaccharide units with a β-1,4-linked D-glucose backbone and trisaccharide side chains composed of mannose-(β-1,4)-glucuronic acid-(β-1,2)-mannose attached to alternate glucose residues in the backbone by α-1,3 linkages (Jansson *et al.*, 1975). Mannose residues are acetylated and pyruvylated at specific sites (Stankowski *et al.*, 1993). Xanthan biosynthesis involves the assembly of a pentasaccharide repeating unit attached to an inner membrane polyprenol phosphate carrier via the sequential transfer of monosaccharides from sugar nucleotides by glycosyltransferases, and the subsequent polymerization of the pentasaccharide repeating units and secretion (Ielpi *et al.*, 1993) (Fig. S1, see Supporting Information).

In this work, the participation of *oprB* in Xcc biofilm formation and bacterial virulence was analysed, together with its role as a glucose transport protein. In addition, changes in EPS production in response to impaired glucose uptake were evaluated and discussed with a view to gain further insight into the pathogenicity process of this plant pathogen.

RESULTS

OprB is an outer membrane protein

OprB is predicted to be an outer membrane protein by PSORTb 3.0 (Yu *et al.*, 2010) with a score of 9.92/10. To further confirm that it is located in the bacterial outer membrane, an Xcc outer membrane protein extract was obtained and proteins were submitted to mass spectrometry (MS) to determine the presence of OprB in these membranes. A total of 44 proteins were identified, most belonging to the bacterial outer membrane. Among the identified proteins, OprB was found from which three peptides were identified observed in 46 peptide spectrum matches (Table 1). These results corroborate the presence of OprB in the Xcc outer membrane.

OprB is required for Xcc biofilm formation

To investigate the role of OprB in Xcc biofilm formation, a mutant named XccΔoprB was constructed by plasmid integration. For use as a control, a complemented mutant strain was obtained by conjugating a replicative vector, pBBR1MCS-3, carrying a full-length copy of *oprB*, into XccΔoprB, generating XccΔoprBc. Xcc, XccΔoprB and XccΔoprBc were cultured statically in 24-well polyvinyl chloride (PVC) plates in XVM2 medium. After 7 days, Xcc and XccΔoprBc were able to form bacterial aggregates, whereas the mutant was not (data not shown). After 7, 10 and 14 days of growth, biofilms were collected and quantified by serial dilution. The initial population was around 10^9 colony-forming units (cfu)/mL for the three strains. However, after 14 days of culture, Xcc and XccΔoprBc reached cell densities of 8×10^{10} and 6×10^9 cfu/mL, respectively, whereas XccΔoprB did not grow and the population decreased to 3×10^7 cfu/mL (Fig. 1A). In addition, the growth rates of the three strains in Nutrient Broth (NB), Silva–Buddenhagen (SB) and XVM2 media under agitation were analysed. In the three media, XccΔoprB grew less than the wild-type strain and the complemented strain at the initial stages of growth, but at the early stationary phase they achieved the same population (Fig. S2, see Supporting Information).

To assess biofilm formation, the strains were grown statically in borosilicate glass tubes in XVM2 medium for 7, 10 and 14 days. Staining of bacterial cells with crystal violet (CV) stain showed that, under these conditions, Xcc and XccΔoprBc produced biofilms of cells that adhered to the glass surface, forming a thick ring at the air–liquid interface of the culture medium, whereas the XccΔoprB mutant was altered in its ability to form such a structure and only formed a narrow ring of cells (Fig. 1B). CV staining of Xcc and XccΔoprBc strains was over three times greater than that of the XccΔoprB mutant ($P < 0.05$) at the time points analysed (Fig. 1C). These results indicate that the loss of OprB compromises the Xcc biofilm formation process.

Table 1 Identification of OprB (Outer membrane protein B) in *Xanthomonas citri* ssp. *citri* (Xcc) outer membranes.

Peptide sequence	MH^+ (Da)	Protein	Peptide spectrum match	Protein group accession
IAPNLHYVINPDQFNEPTR	2238.13199	1	4	OprB (Q8PJM6)
NALIAGMR	845.46630	1	5	OprB (Q8PJM6)
YSDEAIENLR	1209.57512	1	37	OprB (Q8PJM6)

Differences in statically growing cells were also analysed by confocal laser scanning microscopy using a green fluorescent protein (GFP)-expressing XccΔoprB mutant strain. A complemented GFP-expressing XccΔoprBc strain could not be constructed as it already bears a pBBR1MCS-3 plasmid. The previously constructed GFP-expressing Xcc (Gottig *et al.*, 2009) and the GFP-expressing XccΔoprB mutant were cultured in static liquid XVM2 medium in 24-well PVC plates. After 7 days, microscopic analysis showed the typical biofilm structure formed by large cell cumuli in Xcc (Zimaro *et al.*, 2014), whereas XccΔoprB showed no such structures. Bacterial biofilm lengths were analysed by capturing serial images at 0.5-μm intervals (*z*-stack) covering the entire well length. The results revealed that Xcc formed the typical thick bacterial biofilm of about 240 μm in depth (Zimaro *et al.*, 2014), whereas the mutant formed thinner biofilms of 50 μm (Fig. 1D).

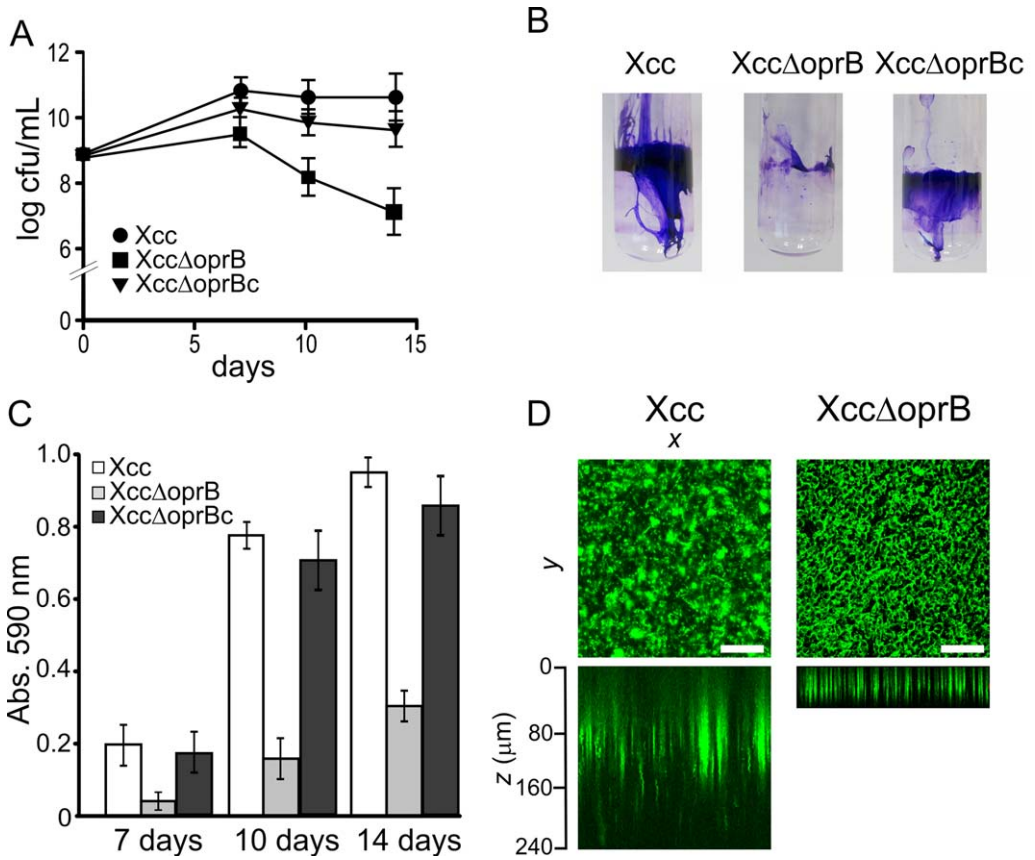

Fig. 1 Biofilm formation of *Xanthomonas citri* ssp. *citri* (Xcc), XccΔoprB and XccΔoprBc strains. (A) Population size of the biofilm fraction of bacteria incubated statically at 28°C. The results are the means of three independent experiments in which each strain was analysed five times. Error bars are standard deviations. The data were statistically analysed using one-way analysis of variance (ANOVA) ($P < 0.05$). cfu, colony-forming units. (B) Representative photographs of biofilm formation assay for Xcc, XccΔoprB and XccΔoprBc strains grown statically in borosilicate glass tubes during 10 days in XVM2 medium and stained with crystal violet (CV). (C) Quantification of the CV retained by the adhered cells at the time points stated. CV stain was measured spectrophotometrically (absorbance at 590 nm). Bars represent the means of the quantification of five tubes for each strain. The results are representative of three independent experiments. Error bars are standard deviations. The data were statistically analysed using one-way ANOVA ($P < 0.05$). (D) Representative photographs of laser scanning confocal analysis of green fluorescent protein (GFP)-expressing Xcc and XccΔoprB strains cultured in static liquid XVM2 in 25-well PVC plates during 7 days (top), and serial images taken at 0.5-μm distances (*z*-stack) (bottom).

The porin OprB is required for virulence, affecting host tissue attachment, canker development and epiphytic survival

We investigated the importance of OprB for the virulence of Xcc on *Citrus sinensis* plants. Given the observed differences in bacterial adherence to PVC and glass surfaces, we tested whether XccΔoprB shows impaired ability to adhere to the leaf surface, using CV staining to measure bacterial attachment. Xcc and XccΔoprBc were able to adhere to the leaf tissue, as observed previously for the wild-type strain (Zimaro *et al.*, 2014), whereas the XccΔoprB mutant could not adhere, shown by the absence of CV staining (Fig. 2A,B). These results indicate that OprB is required for leaf surface attachment.

We then determined the ability of the XccΔoprB mutant to cause disease in citrus plants. The Xcc, XccΔoprB and XccΔoprBc strains were pressure infiltrated into citrus leaves at a concentration of 10^7 cfu/mL. No differences in the onset or size of the lesions, or in bacterial growth, were observed between the three strains (data not shown). However, when the bacterial strains were either infiltrated at a concentration of 10^5 cfu/mL, which allows the observation of canker lesions, or spray inoculated, resembling natural infection, the XccΔoprB mutant strain showed a significantly lower ($P < 0.05$) number of canker lesions formed, with 50% fewer lesions than on leaves inoculated with Xcc wild-type or complemented strains (Fig. 2C,D). To evaluate the role of OprB in bacterial growth inside the host, the populations of Xcc, XccΔoprB and XccΔoprBc infiltrated at a concentration of 10^5 cfu/mL in citrus leaves were quantified (Fig. 2E). The results showed that the number of XccΔoprB bacteria recovered from the infected leaves was significantly lower than that of the wild-type, whereas no significant differences between the growth of XccΔoprBc and the wild-type bacteria were observed.

Moreover, the epiphytic survival of bacteria inoculated onto citrus leaves by spraying was evaluated. By 7 days post-inoculation (dpi), the population size of Xcc wild-type bacteria and XccΔoprBc had decreased about 10-fold ($P < 0.05$), whereas the population size of the XccΔoprB mutant was about 80 times lower than the starting inoculum ($P < 0.05$) (Fig. 2F). By 21 dpi, only 0.1% of the initial XccΔoprB inoculum survived, compared with 6% and 2% for the Xcc wild-type and the complemented strains, respectively ($P < 0.05$) (Fig. 2F). Together, these results suggest that OprB plays an important role in Xcc fitness.

OprB is required for bacterial growth in glucose and sucrose, and for glucose uptake

Given that OprB has been implicated in carbon metabolism, specifically in carbohydrate transport in other bacteria, we investigated whether the mutation in *oprB* in Xcc has an effect on the growth of Xcc cells on different carbon sources. Xcc, XccΔoprB and XccΔoprBc were grown in M9 minimal medium supplemented with 0.5% (w/v) glucose, fructose, sucrose or succinate as the sole carbon source. In the presence of glucose or sucrose, the cell densities of the wild-type and complemented strains showed 10^4 and 10^3 times greater increase, respectively, than that of the mutant strain ($P < 0.05$) (Fig. 3A). There were no significant differences between the strains in their growth on either fructose or succinate (Fig. 3A). These results suggest that OprB is required for optimal growth on glucose and sucrose, but not for growth on the organic acid succinate, probably acting as a carbohydrate-selective porin.

The orthologous OprB protein in *P. aeruginosa* is described as a carbohydrate transporter (Wylie and Worobec, 1995), with evidence that it specifically transports glucose (van den Berg, 2012). Therefore, we tested whether Xcc OprB has the capacity to transport glucose by [^{14}C]glucose uptake assays with Xcc wild-type, XccΔoprB and XccΔoprBc grown in XVM2 medium. The rate of glucose uptake by the XccΔoprB mutant strain, which lacks OprB, was about 60% lower than that by the wild-type when 1 μM [^{14}C]glucose was supplied exogenously (Fig. 3B). Kinetic analysis with external glucose concentrations ranging from 0.1 to 4.0 μM indicated maximal rates of glucose uptake of 32.3 and 29.7 μmol/min for the wild-type Xcc and complemented strains, respectively, whereas the maximal rate for the XccΔoprB mutant was 17.5 μmol/min.

The lack of OprB enhances Xcc xanthan production, increases its viscosity and modifies the pattern of xanthan pyruvylation

XccΔoprB mutant colonies were more mucoid than Xcc colonies (data not shown); therefore, the production of xanthan was measured in Xcc, XccΔoprB and XccΔoprBc. The lack of *oprB* increased EPS production over two-fold compared with the wild-type Xcc ($P < 0.05$) in bacteria grown in XOL medium supplemented with 4% (w/v) glucose (Fig. 4A). Similarly, the mutant also produced about twice as much EPS as wild-type Xcc when glucose was replaced with sucrose or fructose. When succinate was used as carbon source, no differences were observed in the amount of EPS produced among strains. It is worth mentioning that supplementation of XOL with 4% succinate was lethal for Xcc strains; therefore, the assay was performed with 1% (Fig. 4A). Expression of the sugar transferase gene *gumD*, which encodes the first enzyme in the xanthan biosynthetic pathway, was over five times higher in XccΔoprB relative to the wild-type and complemented strains ($P < 0.05$) (Fig. S3, see Supporting Information). Taking into account the differences observed in Xcc and XccΔoprB growth in different culture media (Fig. S1), we measured the bacterial population at different time points in XOL medium supplemented with glucose. At every time point analysed, the population sizes of Xcc and XccΔoprBc were larger than that of XccΔoprB (data not shown) and, at 96 h, the time at which xanthan was quantified,

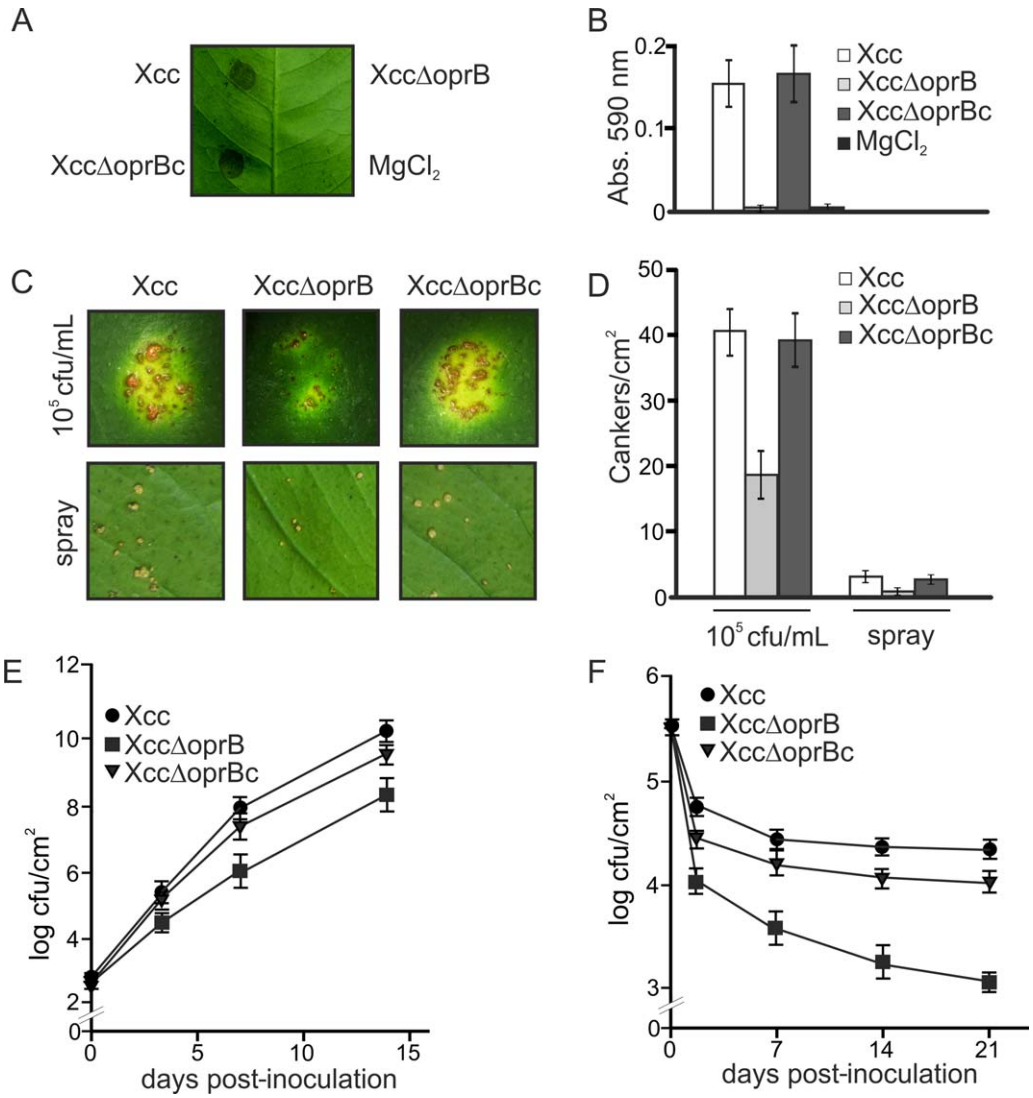

Fig. 2 Bacterial adherence, virulence and epiphytic survival of *Xanthomonas citri* ssp. *citri* (Xcc), XccΔoprB and XccΔoprBc in citrus leaves. (A) Representative photograph of Xcc, XccΔoprB and XccΔoprBc adhered to the abaxial leaf surface and stained with crystal violet (CV). As a control, 10 mM $MgCl_2$ was used. (B) Quantitative measurement of the CV retained by Xcc, XccΔoprB and XccΔoprBc cells and the control. Bars represent the mean of the quantified CV stain from eight stained leaf spots of each strain measured spectrophotometrically (absorbance at 590 nm). Error bars are standard deviations. The results are representative of three independent experiments. (C) Representative photographs of Xcc, XccΔoprB and XccΔoprBc inoculated by pressure infiltration (top) or sprayed (bottom) on the abaxial surface of citrus leaves. (D) Canker lesion quantification for the experiments performed as in (C), presented as cankers per square centimetre of leaf tissue. At least six leaves were analysed in all cases and the experiment was repeated three times. Error bars are standard deviations. The data were statistically analysed using one-way analysis of variance (ANOVA) ($P < 0.05$). (E) Bacterial growth of Xcc, XccΔoprB and XccΔoprBc in citrus leaves infiltrated as described in (C) at 10^5 colony-forming units (cfu)/mL; values represent the means of three samples and error bars are standard deviations. (F) Xcc, XccΔoprB and XccΔoprBc were sprayed onto citrus leaves and the population sizes of the bacteria that survived epiphytically at the stated time points were calculated as log cfu/cm^2. Each data point is the mean of four leaves assayed for each strain; the results are representative of three independent experiments. Error bars are standard deviations. The data were statistically analysed using one-way ANOVA ($P < 0.05$).

the Xcc population was 1.2×10^{15} cfu/mL, whereas that of XccΔoprB was 3.2×10^{13} (Fig. 4B).

The viscosity of EPS can be related to the quality of the polymer (i.e. longer chains) (Galvan *et al.*, 2013). The XccΔoprB mutant showed an increase of 48% in EPS low shear rate viscosity compared with Xcc (Fig. 4B), suggesting that some change in the quality of xanthan is produced by Xcc cells that lack OprB. Samples of the xanthan EPS produced by the Xcc and XccΔoprB strains were acid hydrolysed and analysed by ^{1}H-nuclear magnetic resonance (NMR) spectroscopy. The spectral peaks representing

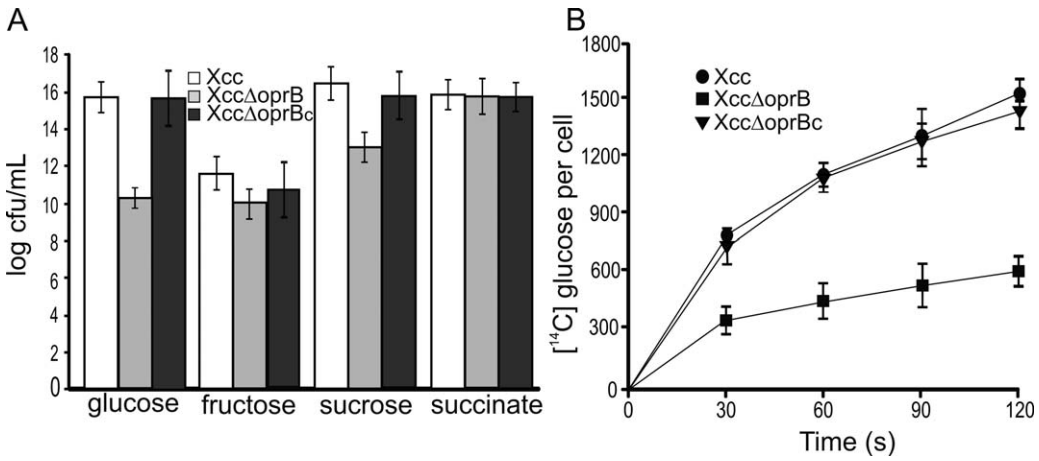

Fig. 3 Analysis of *Xanthomonas citri* ssp. *citri* (Xcc), XccΔoprB and XccΔoprBc growth in different carbon sources and [^{14}C]glucose uptake by the different Xcc strains. (A) Growth of Xcc, XccΔoprB and XccΔoprBc in M9 medium containing 0.5% (w/v) glucose, fructose, sucrose and succinate at 24 h. Each bar represents the mean of five independent experiments. Error bars are standard deviations. The data were statistically analysed using one-way analysis of variance (ANOVA) ($P < 0.05$). cfu, colony-forming units. (B) Import of 1 μM glucose over 120 s by Xcc, XccΔoprB and XccΔoprBc. Each data point represents the mean of three independent experiments. Error bars are standard deviations. The data were statistically analysed using one-way ANOVA ($P < 0.05$).

the glucose, mannose and glucuronic acid moieties of xanthan were almost identical for xanthan extracted from the two strains (Fig. 4C). The xanthan from wild-type Xcc also gave a distinct peak for pyruvate, indicating that the Xcc xanthan has a similar composition to that in *X. campestris* pv. *campestris* (Galvan *et al.*, 2013). However, almost no pyruvate was detected in the xanthan from the mutant strain (Fig. 4C), showing that the loss of *oprB* greatly impairs EPS pyruvylation.

Glucose uptake by OprB alters Xcc carbohydrate metabolism

Xcc and XccΔoprB were grown in similar conditions to those in which differences in EPS production between strains were observed, and samples were taken for metabolite analysis. Trehalose-6-phosphate (Tre6P), UDP-glucose (UDPGlc) and glucose-1-phosphate (Glc1P) were significantly increased ($P < 0.05$) in the XccΔoprB mutant strain compared with Xcc (Fig. 5). The other sugar phosphates or glycolytic and tricarboxylic acid cycle intermediates analysed (ADP-glucose, galactose-1-phosphate, glucose-1,6-biphosphate, phosphoenolpyruvate, pyruvate, fructose-6-phosphate, mannose-6-phosphate, maltose-1-phosphate, glyceraldehyde-3-phosphate, succinate and 3-phosphoglycerate) showed no significant differences between the two strains (data not shown).

The outer membrane porin OprB is involved in bacterial stress tolerance

Xcc, XccΔoprB and XccΔoprBc were grown in SB medium to a population of 10^8 cfu/mL and incubated for 15 min with hydrogen peroxide (H_2O_2) at final concentrations of 1–30 mM, and the percentage survival was calculated considering the population present prior to the treatment; 60% of the Xcc population was able to survive at 1 mM H_2O_2, whereas only 6% of the mutant strain survived. Moreover, Xcc tolerated 30 mM H_2O_2 concentration, at which 4% survived, whereas XccΔoprB showed no survival at 5 mM (Fig. 6A). The detergent tolerance was also assayed by incubating the three strains with 0.01% sodium dodecylsulfate (SDS). Xcc achieved 74% survival, but, for XccΔOprB, only 29% survived (Fig. 6B). The complemented XccΔoprBc strain showed similar tolerance to wild-type Xcc to both treatments (Fig. 6).

DISCUSSION

Biofilm lifestyle gives pathogenic bacteria numerous advantages, such as enhanced protection against environmental stresses and increased bacterial resistance against host defence responses, as well as antimicrobial tolerance. The first steps in Xcc pathogenesis are adhesion to the host surface and entry into the host tissue. Once inside the plant apoplast, bacterial aggregation increases the bacterial cell density until a critical mass of bacterial cells is reached at a specific location, enabling the bacteria to initiate and sustain interactions with citrus cells. In addition, epiphytic survival, and hence the possibility of dispersal to new niches, also depends on the ability to aggregate and form biofilms (Gottig *et al.*, 2010). Several Xcc mutants impaired in biofilm formation, such as those with affected EPS, lipopolysaccharide, flagellum or glucan biosynthesis, as well as mutants in the adhesin FhaB and in the two-component regulatory system ColR/ColS, show deficient pathogenesis (Dunger *et al.*, 2007; Gottig *et al.*, 2009; Guo *et al.*, 2010; Li and Wang, 2011b, 2012; Malamud *et al.*, 2011; Petrocelli *et al.*, 2012; Rigano *et al.*, 2007; Yan and Wang, 2011; Yan *et al.*, 2012).

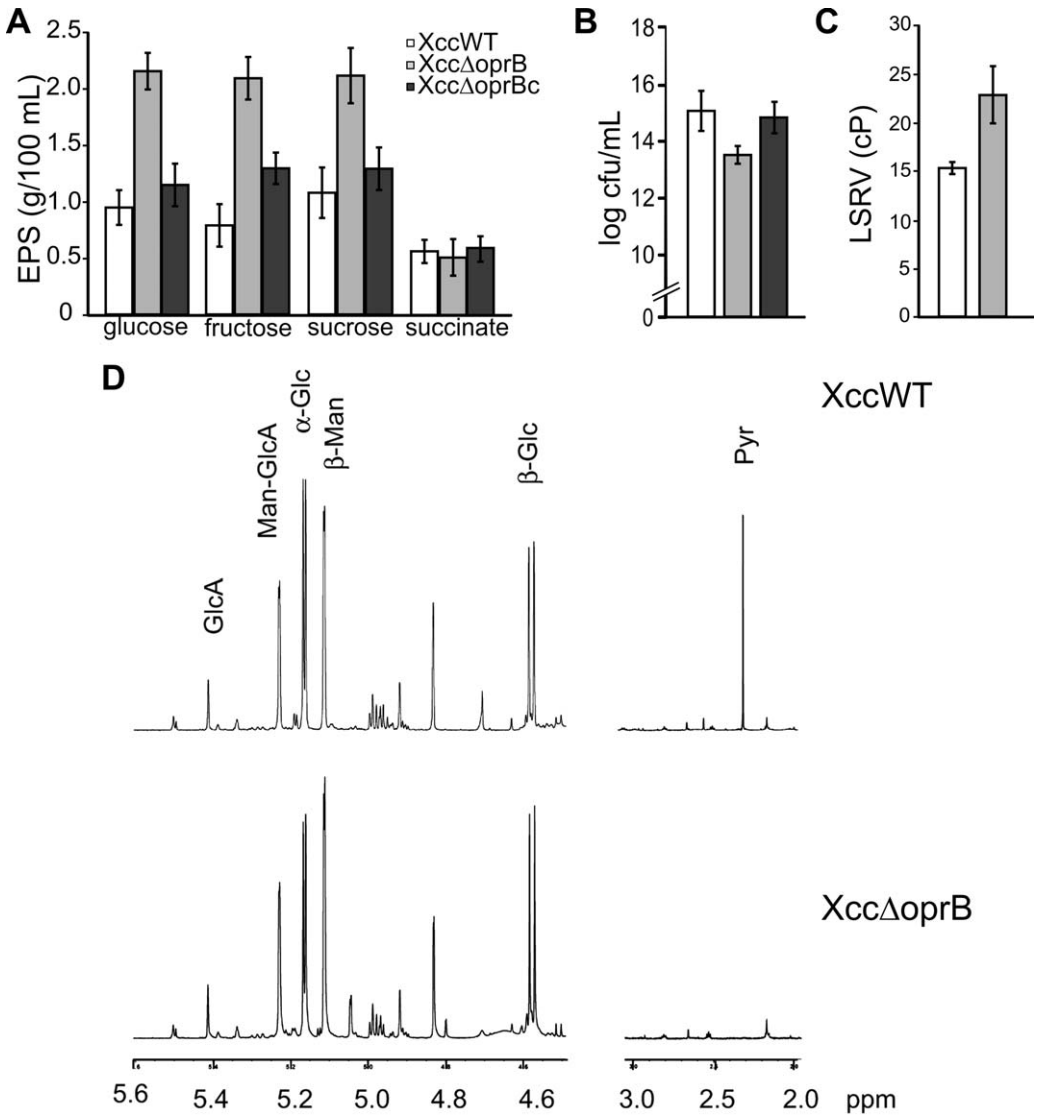

Fig. 4 Xanthan quantification, viscosity and composition in *Xanthomonas citri* ssp. *citri* (Xcc) and derivative strains, and bacterial growth in XOL medium. (A) Extracellular polysaccharide (EPS) present in the supernatant fraction of Xcc, XccΔoprB and XccΔoprBc cultured in XOL supplemented with glucose, fructose, sucrose (4%) or succinate (1%) was precipitated and quantified. Each data point is the mean of the data obtained from three cultures of each strain; the results are representative of three independent experiments. Error bars indicate the standard error. The data were statistically analysed using one-way analysis of variance (ANOVA) ($P < 0.05$). (B) Growth of Xcc, XccΔoprB and XccΔoprBc cultured in XOL supplemented with 4% glucose for 96 h. Each bar represents the mean of three independent experiments. Error bars are standard deviations. The data were statistically analyzed using one-way ANOVA ($P < 0.05$). cfu, colony-forming units. (C) Low shear rate viscosity (LSRV) of xanthan obtained from Xcc and XccΔoprB. Each bar represents the mean of three independent experiments. Error bars are standard deviations. The data were statistically analysed using one-way ANOVA ($P < 0.05$). (D) ^{1}H nuclear magnetic resonance (NMR) of purified xanthan obtained from Xcc and XccΔoprB. The identification of glucose (Glc), mannose (Man), glucuronic acid (GlcA) and pyruvic acid (Pyr) was performed using standard commercial sugars. The peak marked as GlcA corresponds to the lactone form of the molecule obtained under our hydrolysis conditions. Man-GlcA corresponds to the hydrolysis-resistant aldobiuronic acid D-GlcA*p*-β-(1-2)-D-Man*p*.

Furthermore, the use of inhibitors of Xcc biofilm formation has been shown to reduce the number of canker lesions when applied directly on citrus leaf tissue (Li and Wang, 2014). Thus, these examples confirm the importance of biofilm formation in bacterial pathogenicity as a requirement for maximal virulence. A genome-wide-scale analysis using transposon mutagenesis identified several genes already known to be involved in the process of biofilm formation, such as those mentioned above, as well as new ones that need to be studied further (Li and Wang, 2011a). Likewise, proteomic analysis of Xcc cells from biofilms and planktonic cultures revealed a number of proteins that are important for biofilm formation, including OprB (Zimaro *et al.*, 2013). Another

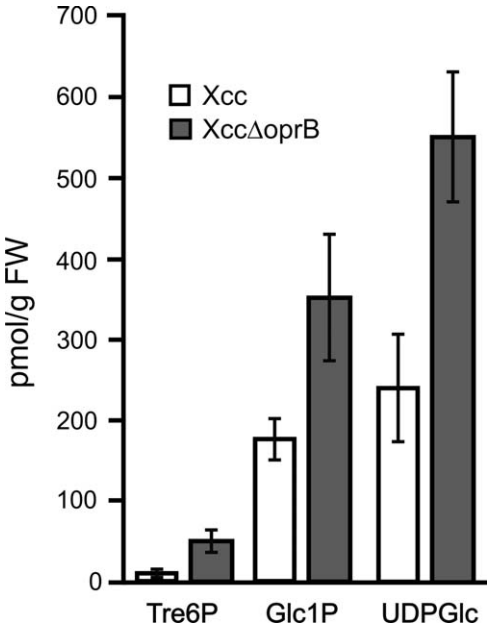

Fig. 5 Metabolite quantification in *Xanthomonas citri* ssp. *citri* (Xcc) and XccΔoprB. Picomoles of the stated metabolites per gram of fresh bacterial weight (FW) were determined. Each data point is the mean of the data obtained from four cultures of each strain. Error bars indicate the standard error. The data were statistically analysed using one-way analysis of variance (ANOVA) ($P < 0.05$). Glc1P, glucose-1-phosphate; Tre6P, trehalose-6-phosphate; UDPGlc, UDP-glucose.

proteomic study found that OprB is more abundant in wild-type Xcc biofilms than in a TTSS mutant that is impaired in biofilm formation (Zimaro *et al.*, 2014), and expression of the *oprB* gene was also enhanced in wild-type Xcc biofilms (Zimaro *et al.*, 2013, 2014). The dependence of biofilm formation on OprB-type proteins has also been demonstrated in *Burkholderia pseudomallei* (Chan and Chua, 2005). In the light of these previous observations, we investigated the role of OprB in Xcc biofilm formation, and thus its importance in bacterial virulence.

Our key findings can be summarized as follows: (i) *oprB* is essential for biofilm formation, as the mutant is impaired in bacterial aggregation and biofilm formation when it is statically grown; (ii) *oprB* is required for bacterial adherence to host tissue, to achieve the maximal number of canker lesions in inoculations with low bacterial concentrations or when spray inoculated, and is also important in epiphytic survival; (iii) OprB is a glucose transporter; (iv) OprB is required for oxidative stress and detergent resistance; and (v) OprB is involved in xanthan production and influences its viscosity and sugar composition, probably by altering the rate of glucose uptake, which has knock-on effects on intracellular glucose metabolism and the production of precursors for xanthan synthesis.

The lack of *oprB* has a deleterious effect on bacterial biofilm formation, adherence to host tissue and epiphytic survival, all crucial steps in pathogenesis. Considering the importance of sugar uptake to complete the disease cycle, the shortage of glucose uptake may indicate a status in which the bacteria cannot form biofilm structures and must remain in a planktonic state to colonize new niches (Gottig *et al.*, 2010). In addition, the impairment in glucose uptake of the *oprB* mutant renders the bacteria less virulent. This is consistent with the requirement for nutrient acquisition from the leaf to establish the infection, such that the mutant showed reduced symptoms compared with the more virulent wild-type Xcc. This effect has been observed previously in *Xanthomonas* mutants with reduced ability to utilize carbohydrates (Blanvillain *et al.*, 2007; Lu *et al.*, 2009). It is important to note that differences in virulence were observed only with Xcc bacterial concentrations lower than 10^7 cfu/mL. These results suggest that, at low bacterial concentrations, as would usually be the case in natural infections, the lack of glucose uptake and biofilm formation is detrimental for disease development. The *oprB* mutant also showed increased sensitivity to H_2O_2 and the detergent SDS. H_2O_2 is the main component of the plant oxidative burst during plant–pathogen interactions, and thus OprB may also be involved in

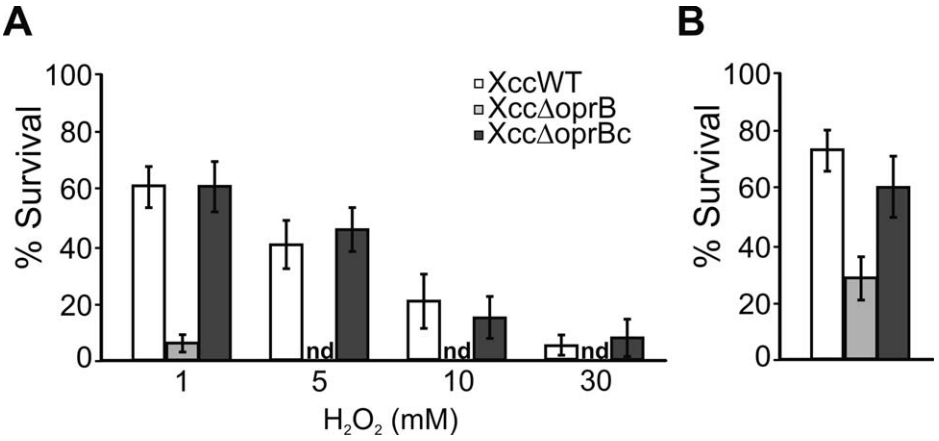

Fig. 6 Survival of *Xanthomonas citri* ssp. *citri* (Xcc), XccΔoprB and XccΔoprBc exposed to hydrogen peroxide (H_2O_2) and sodium dodecylsulfate (SDS). (A) Survival rate of each strain in the presence of H_2O_2 at the concentrations stated. (B) Survival rate of each strain in the presence of 0.01% SDS. In (A) and (B), **e**ach bar is the mean of three independent experiments in which each strain was evaluated in triplicate. Error bars indicate the standard error. The data were statistically analysed using one-way analysis of variance (ANOVA) ($P < 0.05$).

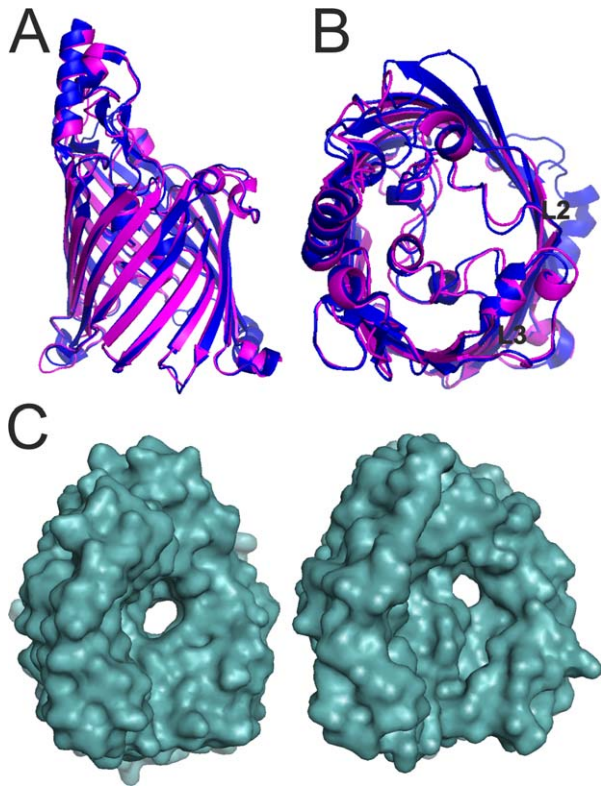

Fig. 7 Modelling of OprB (Outer membrane protein B) structure. Schematic representations of the crystal structures of *Pseudomonas putida* F1 OprB-1 (in purple) and the modelled *Xanthomonas citri* ssp. *citri* (Xcc) OprB (in magenta) viewed from the side (A) and from the extracellular environment (B). Loops 2 (L2) and 3 (L3) are indicated. (C) Pore architecture of F1 OprB-1 (left) and Xcc OprB (right). The structural models were obtained with PyMOL.

adaptation to the plant intercellular space. However, and in view of the infiltration assays, this may occur only at low bacterial concentrations. The lower resistance to SDS of the mutant may also indicate that this porin may function as an efflux pump. Likewise, and considering that SDS resistance is an assay used to evaluate membrane stability, it may be suggested that this outer membrane porin causes structural alterations of the membranes, although this needs to be investigated further.

The homologous OprB protein from *P. putida* F1 (F1-OprB), whose structure has been solved, shows a strong preference for the transport of monosaccharides over disaccharides, with glucose being a preferred substrate (van den Berg, 2012). Modelling of the Xcc OprB on the *P. putida* (4GEY) protein structure (van den Berg, 2012) suggested that it consists of a similar 16-stranded β-barrel with seven extracellular loops (Fig. 7A). Moreover, the regions that line the pore channel and that interact with the glucose molecule in loops 2 and 3 are highly conserved, suggesting that the Xcc OprB has a similarly high specificity for glucose (Fig. 7B). Surface representations of both proteins suggest that they have eyelets with similar architecture (Fig. 7C). In the case of F1-OprB, a preference for monosaccharides was confirmed by liposome swelling experiments, whereas very low transport activities for disaccharides, such as sucrose and maltose, were detected. Loss of OprB in XccΔoprB diminished growth not only on glucose, but also on sucrose. This might indicate that the Xcc OprB has broader substrate specificity than F1-OprB. However, an alternative explanation is that growth on sucrose was dependent on hydrolysis of sucrose to glucose and fructose by secreted invertases, and subsequent uptake of glucose by glucose-specific OprB.

Glucose catabolism in *Xanthomonas* is predominantly performed by the Entner–Doudoroff (ED) pathway, whereas a small portion is routed into the oxidative pentose phosphate pathway and even less by the Embden–Meyerof pathway (Schatschneider *et al.*, 2014). For xanthan biosynthesis, the main precursor is UDPGlc synthesized from UTP and Glc1P by GalU (UTP-glucose-1-phosphate uridylyltransferase) (Wei *et al.*, 1996), and Glc1P is produced by phosphoglucomutase (XanA) from glucose-6-phosphate (Glc6P). It is interesting to note that, in *Xanthomonas oryzae* pv. *oryzae*, the loss of phosphogluconate dehydratase, the central enzyme in the ED pathway that modulates intracellular Glc6P levels, leads to an increase in xanthan production through the change in glucose flux (Kim *et al.*, 2010). Similarly, the increase in xanthan production observed in XccΔoprB may be a consequence of the impairment in glucose uptake, which has the knock-on effect of redistributing carbon flux towards xanthan production. The lack of pyruvylation in the EPS obtained from XccΔoprB may be a result of the use of phosphoenolpyruvate for gluconeogenesis, rather than as a substrate for the enzyme GumL, which catalyses the pyruvylation of the last mannose of the pentasaccharide unit in xanthan polymers (Marzocca *et al.*, 1991). We compared the levels of metabolic intermediates in Xcc and XccΔoprB and observed higher amounts of UDPGlc and Glc1P in the mutant strain. As these metabolites are involved in the first steps of xanthan synthesis, the increase in their concentrations implies that the flux of carbon into xanthan biosynthesis might be increased.

Bacteria must adapt to continuously changing environmental conditions, and usually accumulate carbon and energy reserves to survive periods in which nutrient supply from their environment is temporarily limiting. In this regard, glycogen biosynthesis is a key strategy for such metabolic storage (Wilson *et al.*, 2010). This may be the case when Xcc is grown in XOL medium supplemented with high levels of glucose. By contrast, the impairment in glucose uptake in the XccΔoprB mutant would be expected to modify this balance by diverting energy and carbon intermediates to the synthesis of xanthan. Further, the larger amount of xanthan observed in the mutant strain grown in glucose, but also in sucrose and fructose, might be a result of this carbon redistribution. The decrease in bacterial growth observed in XOL medium with high levels of glucose, and also in other media with lower contents of glucose in the initial growth phases, suggests that wild-type

cultures bearing OprB shoe a better performance with regard to glucose uptake. The major production of EPS observed with glucose, sucrose and fructose, but not with succinate, indicates that the lack of OprB modifies carbohydrate metabolism when sugars are the carbon source, but not with the organic acid succinate, a medium in which XccΔoprB mutant growth is similar to that of Xcc. In support of these changes in bacterial carbohydrate metabolism, the Tre6P content was also increased in the mutant strain. It has been reported that, in several bacteria, such as *Xanthomonas*, glycogen can be converted into trehalose, and that this is a reversible process (Ruhal *et al.*, 2013). Therefore, the differences observed in Tre6P may also be explained by the metabolic reprogramming of the OprB-lacking strain. Therefore, and taking into account the increase in xanthan and Tre6P in the mutant strain, we may hypothesize that the shortage of glucose triggers a reprogramming of carbon metabolism that results in an increased yield of xanthan, which is also modified by a lack of pyruvylation. Overall, these results point to a shift in carbon flux caused by a lack of OprB, which, in turn, influences xanthan production and biofilm formation, although this needs to be investigated further. Although we may expect to observe less xanthan produced by a strain impaired in glucose uptake, the contrary was the case. This may be attributed to the fact that the lack of biofilm formation in the mutant strain probably triggers a deregulation of xanthan production, given that *gumD* expression is also increased in the mutant strain in order to compensate for the lack of the aggregative state. This has been observed previously in another Xcc mutant strain which was unable to form a biofilm, but showed increased xanthan production, as well as XanA and GalU overexpression, compared with Xcc wild-type (Zimaro *et al.*, 2014), and also in an Xcc adhesin deletion mutant (Gottig *et al.*, 2009).

In summary, we have characterized a glucose import protein that is involved in Xcc virulence on citrus, probably by the impairment of nutrient acquisition in the interaction with the host plant tissue. It also plays a role in biofilm formation and EPS production, most probably as a result of modulation of the carbon flux in the bacterial cell. Our results shed light on the linkage between the environmental nutrient availability encountered by a plant pathogen and the physiological responses of the bacterium to colonize the host.

EXPERIMENTAL PROCEDURES

Bacterial strains, culture conditions and media

Xcc, XccΔoprB and XccΔoprBc strains were grown at 28°C in NB (3 g/L beef extract and 5 g/L peptone), SB (5 g/L sucrose, 5 g/L yeast extract, 5 g/L peptone and 1 g/L glutamic acid, pH 7.0), XVM2 medium [20 mM NaCl, 10 mM $(NH_4)_2SO_4$, 1 mM $CaCl_2$, 0.01 mM $FeSO_4$, 5 mM $MgSO_4$, 0.16 mM KH_2PO_4, 0.32 mM K_2HPO_4, 10 mM fructose, 10 mM sucrose and 0.03% casein acid hydrolysate (casaminoacids), pH 6.7], M9 medium (25 mM KH_2PO_4, 50 mM Na_2HPO_4, 10 mM NaCl, 18.6 mM NH_4Cl, 1 mM $MgCl_2$, 0.2 mM $CaCl_2$, pH 7) or XOL medium [4 mM K_2HPO_4, 1.5 mM KH_2PO_4, 7.6 mM $(NH_4)_2SO_4$, 66 μM $FeSO_4$, 5 mM $MnCl_2$, 0.5 mM $MgCl_2$, 1.25 g/L tryptone, 1.25 g/L yeast extract and 4% (w/v) glucose]. Unless indicated otherwise, the strains were grown with constant agitation at 200 rpm on a rotating shaker. Antibiotics were used at the following final concentrations: ampicillin (Ap), 25 mg/mL; kanamycin (Km), 40 mg/mL; tetracycline (Tc), 15 mg/mL. The wild-type Xcc strain used in this work is named Xcc99-1330 and was kindly provided by Blanca I. Canteros (INTA Bella Vista, Argentina). The XccΔoprB mutant was obtained by plasmid integration; the mid-portion of *oprB* was amplified by polymerase chain reaction (PCR) using the following primers: oprB Up, 5′-CGC*GGATCC*C AACTCGGCCTGCGGCAACC-3′; oprB Down, 5′-CCC*AAGCTT*ATGAAAT GGTCCTCGATCGC-3′. The restriction sites for *Bam*HI and *Hind*III, respectively, are shown in italic type. Amplified products were cloned in the suicide vector pK19mobGII (Katzen *et al.*, 1999) previously digested with the same enzymes. *Escherichia coli* S17-1 cells transformed with this vector were conjugated to Xcc and selected for Km resistance to obtain the XccΔoprB mutant, as described in Sgro *et al.* (2012). The XccΔoprBc complemented strain was constructed by cloning the *oprB* gene in the replicative plasmid pBBR1MCS-3 (Kovach *et al.*, 1995) under the control of the *lacZ* promoter. This region was amplified from Xcc genomic DNA by PCR using the following primers: oprBc Up, 5′-CGC*GGTACC*GATGATCGAC GGCGGCCGCAA-3′; oprBc Down, 5′-TCC*CCCGGG*TCACAGATTCCAGTCG ATCC-3′. It was cloned into pBBR1MCS-3 previously digested with the restriction enzymes *Kpn*I and *Sma*I (italic type). The resulting plasmid was electroporated into the XccΔoprB strain and the complemented mutant strain was selected by growth on Tc-containing medium.

Preparation of Xcc outer cell membrane proteins

Xcc was grown to an optical density of 0.8 in XVM2 4% glucose. Bacteria were centrifuged at 5000 ***g*** for 10 min at 4°C and the pellet was washed twice with phosphate-buffered saline (PBS). Cells were suspended in PBS, 0.1 mM phenylmethylsulfonylfluoride (PMSF) and 1 mM dithiothreitol (DTT), disrupted by sonication and centrifuged at 5000 ***g*** for 10 min at 4°C to remove unbroken cells and cellular debris. The supernatant was incubated with 2.2% sodium sarcosinate (final concentration) and cell envelopes were recovered by ultracentrifugation at 100 000 ***g*** for 45 min at 4°C. The pellet was resuspended in 100 μL of 20 mM tris(hydroxymethyl)aminomethane (Tris)-HCl (pH 8), 1 mM ethylenediaminetetraacetic acid (EDTA) and 1% SDS; 10 mM DTT was added and incubated at 56°C for 45 min. Freshly prepared 20 mM iodoacetamide was added and further incubated in the dark for 45 min. Final precipitation was performed by adding 16% trichloroacetic acid (TCA) for 16 h at 4°C. After centrifugation at 15 000 ***g*** for 10 min at 4°C, the pellet was washed twice with cold acetone and air dried.

MS protein identification

Protein digestion and MS analysis were performed at the Proteomics Core Facility CEQUIBIEM at the University of Buenos Aires/CONICET (National Research Council) as follows. The outer membrane protein pellet was resuspended in 50 mM ammonium bicarbonate buffer to achieve a concentration of 20 μg/μL, and digestion was performed with trypsin. After application to a ZipTip C18 pipette tip (Merck Millipore, Darmstadt, Germany) to remove salts, the sample was lyophilized and resuspended in 0.1%

formic acid. The sample was analysed by nano-liquid chromatography-tandem mass spectrometry (nano-LC-MS/MS) in a Thermo Scientific Q Exactive Mass Spectrometer, (Waltham, Massachusetts, USA) ionized by electrospray with EASY-SPRAY. The data-dependent MS2 method was used to fragment the top 12 peaks in each cycle. Data analysis was performed using Proteme Discoverer 1.4 (Thermo Scientific).

Biofilm assays

For *in vitro* biofilm assays, bacteria were grown in SB at 28°C with shaking until the culture reached the exponential growth phase, and then diluted 1 : 10 in fresh XVM2 medium containing appropriate antibiotics. Three millilitres of a diluted bacterial suspension were placed in borosilicate glass tubes and incubated statically for 14 days at 28°C. The population size was estimated by recovering the bacteria present in the biofilm fraction by centrifugation and plating adequate dilutions on SB plates. The quantification of biofilm formation was performed as described previously (O'Toole and Kolter, 1998). The culture medium was poured out and the tubes were washed three times with distilled water to remove non-adherent cells. The cells that remained attached to the tube walls were incubated at 60°C for 10 min and stained with 0.1% CV for 30 min at room temperature. Excess CV was removed by washing under running tap water. Then, the CV stain was solubilized by the addition of 1.5 mL of ethanol–acetone (80 : 20, v/v) to each tube and quantified by measuring the absorbance at 590 nm (Newman *et al.*, 2004).

Confocal analysis of biofilm architecture

An Xcc strain expressing GFP (Gottig *et al.*, 2009) was used to analyse biofilm architecture. The GFP-expressing XccΔoprB strain was obtained by transforming this strain with plasmid pBBR1MCS-5EGFP (Zimaro *et al.*, 2014). GFP-expressing Xcc and XccΔoprB were statically grown in 12-well PVC plates as described above, and biofilm development was analysed after 7 days by confocal laser scanning microscopy (Nikon Eclipse TE-2000-E2, Tokyo, Japan).

Plant material, adhesion assays and inoculations

Citrus sinensis cv. Valencia plants were grown in a growth chamber with incandescent light at 28 °C with a photoperiod of 16 h. Adhesion capacity to leaf surfaces was measured as described previously (Gottig *et al.*, 2009). Cells from overnight cultures of the different strains in XVM2 medium were collected by centrifugation, washed and resuspended in fresh XVM2 to give suspensions with an optical density at 600 nm (OD_{600}) of 0.1. Then, 20 μL of each bacterial suspension were incubated for 6 h at 28°C in a humidified chamber on the abaxial leaf face. Bacterial adhesion was measured by CV staining, with the CV stain being extracted from the bacterial drops by the addition of 95% ethanol and mixing by pipetting up and down with a micropipette. The extracted CV stain was measured spectrophotometrically as described above. For plant inoculation, bacteria were cultured in SB broth to an OD_{600} of 1, harvested by centrifugation and resuspended in 10 mM $MgCl_2$ at 10^5, 10^7 or 10^9 cfu/mL. Two methods of infection were used: (i) infiltration of bacterial suspensions at 10^5 and 10^7 cfu/mL with a needleless syringe; and (ii) spraying bacterial suspensions (10^9 cfu/mL) onto the surface of citrus leaves. Disease symptoms were evaluated every 2 days and canker lesions were counted from six citrus leaves inoculated with the different strains. Leaf area was measured from digitized images using Adobe Photoshop software (San Jose, California, USA).

Quantification of epiphytic growth

Epiphytic fitness was evaluated as described previously (Dunger *et al.*, 2007). Briefly, cells from overnight cultures of the different strains in SB medium were collected by centrifugation, washed and resuspended in 10 mM phosphate buffer (pH 7.0) at a concentration of 10^9 cfu/mL, as described above. The bacterial suspensions were sprayed onto leaves until both leaf surfaces were uniformly wet. Four different leaves inoculated with each strain were taken at different days post-inoculation, cut into pieces with a sterile razor blade and transferred to borosilicate glass tubes with 10 mL of 10 mM potassium phosphate buffer (pH 7.0). Tubes were placed in a Branson model #5510 (Danbury, Connecticut, USA) sonicating water bath for 10 min. Subsequently, each tube was vortexed for 5 s, and serial dilutions were plated on SB plates containing appropriate antibiotics. Colonies were counted after incubation at 28°C for 2 days. The leaf area was quantified by the Image-Pro Program and the bacterial density was expressed as cfu/cm^2 of the inoculated leaves. As a control, *in planta* growth assays were performed by grinding leaf discs from the inoculated leaf in 200 μL of 10 mM $MgCl_2$, diluted and plated to determine cfu/cm^2. We did not recover bacteria from inside of the leaf in the samples.

[^{14}C]Glucose uptake experiments

Pellets of Xcc, XccΔoprB and XccΔoprBc strains grown overnight in XVM2 medium were resuspended in fresh XVM2 and adjusted to an OD_{600} of 1. [^{14}C]Glucose (specific activity, 9.25–13.3 GBq/mmol; Perkin-Elmer, Waltham, Massachusetts, USA) was added to a final concentration of 0.5 μM. The concentration-dependent initial glucose transport was determined with [^{14}C]glucose concentrations ranging from 0.1 to 4 μM. In all cases, samples of 0.2 mL were collected on cellulose nitrate filters at 30, 60, 90 and 120 s, washed twice with water, dried and the radioactivity was determined by liquid scintillation counting.

Quantification of xanthan production, viscosity measurements and xanthan composition

The quantification of xanthan production was performed as described previously (Becker *et al.*, 1998; Dunger *et al.*, 2007). Briefly, bacterial strains were cultured to the stationary growth phase at 28°C in 50 mL of XOL liquid medium supplemented with 4% (w/v) glucose or sucrose in 250-mL flasks, using an orbital shaker rotating at 200 rpm. The cells were removed by centrifugation, the supernatant fluids were supplemented with KCl at 1% (w/v) final concentration and 2 vol of ethanol were added. The precipitated crude EPS was collected, washed with ethanol, dried and weighed. Low shear rate viscosity measurements of 0.45% xanthan solutions in synthetic tap water (16.2 mM NaCl, 0.95 mM $CaCl_2$) were performed using a Brookfield viscometer (Middleboro, Massachusetts, USA) (RVTD II), as described by Galvan *et al.* (2013). For analyses of xanthan composition, EPS isolated from culture supernatants was hydrolysed in 2 M trifluoroacetic acid at 120 °C for 90 min. The chemical composition of the hydrolysed samples (glucose, mannose, glucuronate and pyruvate) was determined by ^{1}H NMR, with NMR spectra being collected at 298 K

on a Bruker Avance® 600-MHz spectrometer (Billerica, Massachusetts, USA) equipped with a triple-resonance cryoprobe.

Quantification of bacterial metabolites

Xcc and XccΔoprB bacterial strains were cultured in XOL medium at 28°C for 96 h. Cells from 3 mL of bacterial culture were collected by centrifugation, the supernatant was discarded and the mass of the cells was determined by weighing. Cells were washed twice with 15 mM NaCl, before the addition of 300 μL of ice-cold $CHCl_3/CH_3OH$ (3 : 7, v/v) and thorough mixing. Samples were sonicated in ice and incubated at −20°C for 2 h with repeated agitation. Water (300 μL) was added to each sample, followed by thorough mixing and centrifugation at 420 ***g*** for 5 min to separate the phases. The upper aqueous phase was transferred to a new tube and the lower chloroform phase was re-extracted with 300 μL of water. The two aqueous phases were combined and evaporated to dryness using a centrifugal vacuum dryer. Metabolites were measured by high-performance anion-exchange LC-MS/MS, as described previously (Lunn *et al.*, 2006).

Survival on H_2O_2 exposure

Survival experiments on exposure to H_2O_2 were performed by subculture of overnight cultures of the different strains into fresh SB medium at 2% inoculum. After 24 h of growth, aliquots of the cultures were diluted and plated on SB-agar plates to quantify the number of cfu/mL. H_2O_2 was then added to the cultures at final concentrations of 1–30 mM. After 15 min of exposure to the oxidant, samples were removed, washed once with fresh medium, serially diluted and plated on SB-agar plates to quantify the number of cfu/mL. The percentage survival was calculated as the number of cfu/mL after treatment divided by the number of cfu/mL prior to treatment × 100.

Survival on exposure to SDS

Survival experiments on exposure to SDS were analysed by subculture of 24-h cultures into fresh SB medium at 2% inoculum, with and without the addition of SDS to a final concentration of 0.01%. These cultures were grown for 24 h with shaking at 28°C and the number of cfu/mL was quantified by plating an adequate bacterial dilution on SB plates. The percentage survival was calculated as the number of cfu/mL in the presence of SDS treatment divided by the number of cfu/mL in the absence of SDS treatment × 100.

ACKNOWLEDGEMENTS

We thank Catalina Anderson (INTA Concordia, Argentina), Gastón Alanis and Rubén Díaz Vélez (Proyecto El Alambrado, Entre Rios, Argentina) for the citrus plants, Diego Aguirre [Instituto de Biología Molecular y Celular de Rosario, Consejo Nacional de Investigaciones Científicas y Técnicas (IBR-CONICET), Rosario, Argentina] for plant technical assistance, and Clara Smal and Martìn Aran (Instituto Leloir, Buenos Aires, Argentina) for their assistance with the NMR experiments. This work was supported by grants from Agencia Nacional de Promoción Científica y Tecnológica (PICT2013-0625). EMG, LI, NG and JO are staff members and FAF and CG are fellows of the Consejo Nacional de Investigaciones Científicas y Técnicas (CONICET).

REFERENCES

An, S.Q., Febrer, M., McCarthy, Y., Tang, D.J., Clissold, L., Kaithakottil, G., Swarbreck, D., Tang, J.L., Rogers, J., Dow, J.M. and Ryan, R.P. (2013) High-resolution transcriptional analysis of the regulatory influence of cell-to-cell signalling reveals novel genes that contribute to Xanthomonas phytopathogenesis. *Mol. Microbiol.* **88**, 1058–1069.

Barber, C.E., Tang, J.L., Feng, J.X., Pan, M.Q., Wilson, T.J., Slater, H., Dow, J.M., Williams, P. and Daniels, M.J. (1997) A novel regulatory system required for pathogenicity of *Xanthomonas campestris* is mediated by a small diffusible signal molecule. *Mol. Microbiol.* **24**, 555–566.

Becker, A., Katzen, F., Puhler, A. and Ielpi, L. (1998) Xanthan gum biosynthesis and application: a biochemical/genetic perspective. *Appl. Microbiol. Biotechnol.* **50**, 145–152.

van den Berg, B. (2012) Structural basis for outer membrane sugar uptake in pseudomonads. *J. Biol. Chem.* **287**, 41 044–41 052.

Blanvillain, S., Meyer, D., Boulanger, A., Lautier, M., Guynet, C., Denance, N., Vasse, J., Lauber, E. and Arlat, M. (2007) Plant carbohydrate scavenging through tonB-dependent receptors: a feature shared by phytopathogenic and aquatic bacteria. *PLoS One*, **2**, e224.

Brunings, A.M. and Gabriel, D.W. (2003) *Xanthomonas citri*: breaking the surface. *Mol. Plant Pathol.* **4**, 141–157.

Chan, Y.Y. and Chua, K.L. (2005) The *Burkholderia pseudomallei* BpeAB-OprB efflux pump: expression and impact on quorum sensing and virulence. *J. Bacteriol.* **187**, 4707–4719.

Dow, J.M., Feng, J.X., Barber, C.E., Tang, J.L. and Daniels, M.J. (2000) Novel genes involved in the regulation of pathogenicity factor production within the *rpf* gene cluster of *Xanthomonas campestris*. *Microbiology*, **146**, 885–891.

Dunger, G., Relling, V.M., Tondo, M.L., Barreras, M., Ielpi, L., Orellano, E.G. and Ottado, J. (2007) Xanthan is not essential for pathogenicity in citrus canker but contributes to Xanthomonas epiphytic survival. *Arch. Microbiol.* **188**, 127–135.

Galvan, E.M., Ielmini, M.V., Patel, Y.N., Bianco, M.I., Franceschini, E.A., Schneider, J.C. and Ielpi, L. (2013) Xanthan chain length is modulated by increasing the availability of the polysaccharide copolymerase protein GumC and the outer membrane polysaccharide export protein GumB. *Glycobiology*, **23**, 259–272.

Gottig, N., Garavaglia, B.S., Garofalo, C.G., Orellano, E.G. and Ottado, J. (2009) A filamentous hemagglutinin-like protein of *Xanthomonas axonopodis* pv. *citri*, the phytopathogen responsible for citrus canker, is involved in bacterial virulence. *PLoS One*, **4**, e4358.

Gottig, N., Garavaglia, B.S., Garofalo, C.G., Zimaro, T., Sgro, G.G., Ficarra, F.A., Dunger, G., Daurelio, L.D., Thomas, L., Gehring, C., Orellano, E.G. and Ottado, J. (2010) Mechanisms of infection used by *Xanthomonas axonopodis* pv. *citri* in citrus canker disease. In: Current Research, Technology and Education Topics in Applied Microbiology and Microbial Biotechnology (Méndez-Vilas, A., ed.), pp. 196–204 Formatex Research Center.

Graham, J.H., Gottwald, T.R., Cubero, J. and Achor, D.S. (2004) *Xanthomonas axonopodis* pv. *citri*: factors affecting successful eradication of citrus canker. *Mol. Plant Pathol.* **5**, 1–15.

Guo, Y., Sagaram, U.S., Kim, J.S. and Wang, N. (2010) Requirement of the *galU* gene for polysaccharide production by and pathogenicity and growth *in planta* of *Xanthomonas citri* subsp. *citri*. *Appl. Environ. Microbiol.* **76**, 2234–2242.

Guo, Y., Zhang, Y., Li, J.L. and Wang, N. (2012) Diffusible signal factor-mediated quorum sensing plays a central role in coordinating gene expression of *Xanthomonas citri* subsp. *citri*. *Mol. Plant–Microbe Interact.* **25**, 165–179.

Ielpi, L., Couso, R.O. and Dankert, M.A. (1993) Sequential assembly and polymerization of the polyprenol-linked pentasaccharide repeating unit of the xanthan polysaccharide in *Xanthomonas campestris*. *J. Bacteriol.* **175**, 2490–2500.

Jansson, P.E., Kenne, L. and Lindberg, B. (1975) Structure of extracellular polysaccharide from *Xanthomonas campestris*. *Carbohydr. Res.* **45**, 275–282.

Katzen, F., Becker, A., Ielmini, M.V., Oddo, C.G. and Ielpi, L. (1999) New mobilizable vectors suitable for gene replacement in gram-negative bacteria and their use in mapping of the 3′ end of the *Xanthomonas campestris* pv. campestris gum operon. *Appl. Environ. Microbiol.* **65**, 278–282.

Kim, S.Y., Lee, B.M. and Cho, J.Y. (2010) Relationship between glucose catabolism and xanthan production in *Xanthomonas oryzae* pv. *oryzae*. *Biotechnol. Lett.* **32**, 527–531.

Kovach, M.E., Elzer, P.H., Hill, D.S., Robertson, G.T., Farris, M.A., Roop, R.M. II. and Peterson, K.M. (1995) Four new derivatives of the broad-host-range cloning vector pBBR1MCS, carrying different antibiotic-resistance cassettes. *Gene*, **166**, 175–176.

Li, J. and Wang, N. (2011a) Genome-wide mutagenesis of *Xanthomonas axonopodis* pv. *citri* reveals novel genetic determinants and regulation mechanisms of biofilm formation. *PLoS One*, **6**, e21804.

Li, J. and Wang, N. (2011b) The wxacO gene of *Xanthomonas citri* ssp. *citri* encodes a protein with a role in lipopolysaccharide biosynthesis, biofilm formation, stress tolerance and virulence. *Mol. Plant Pathol.* **12**, 381–396.

Li, J. and Wang, N. (2012) The gpsX gene encoding a glycosyltransferase is important for polysaccharide production and required for full virulence in *Xanthomonas citri* subsp. *citri*. *BMC Microbiol.* **12**, 31.

Li, J. and Wang, N. (2014) Foliar application of biofilm formation inhibiting compounds enhances control of citrus canker caused by *Xanthomonas citri* subsp. *citri*. *Phytopathology*, **104**, 134–142.

Lu, G.T., Xie, J.R., Chen, L., Hu, J.R., An, S.Q., Su, H.Z., Feng, J.X., He, Y.Q., Jiang, B.L., Tang, D.J. and Tang, J.L. (2009) Glyceraldehyde-3-phosphate dehydrogenase of *Xanthomonas campestris* pv. campestris is required for extracellular polysaccharide production and full virulence. *Microbiology*, **155**, 1602–1612.

Lunn, J.E., Feil, R., Hendriks, J.H., Gibon, Y., Morcuende, R., Osuna, D., Scheible, W.R., Carillo, P., Hajirezaei, M.R. and Stitt, M. (2006) Sugar-induced increases in trehalose 6-phosphate are correlated with redox activation of ADPglucose pyrophosphorylase and higher rates of starch synthesis in *Arabidopsis thaliana*. *Biochem. J.* **397**, 139–148.

Malamud, F., Torres, P.S., Roeschlin, R., Rigano, L.A., Enrique, R., Bonomi, H.R., Castagnaro, A.P., Marano, M.R. and Vojnov, A.A. (2011) The *Xanthomonas axonopodis* pv. *citri* flagellum is required for mature biofilm and canker development. *Microbiology*, **157**, 819–829.

Marzocca, M.P., Harding, N.E., Petroni, E.A., Cleary, J.M. and Ielpi, L. (1991) Location and cloning of the ketal pyruvate transferase gene of *Xanthomonas campestris*. *J. Bacteriol.* **173**, 7519–7524.

Moreira, L.M., de Souza, R.F., Almeida, N.F., Jr., Setubal, J.C., Oliveira, J.C., Furlan, L.R., Ferro, J.A. and da Silva, A.C. (2004) Comparative genomics analyses of citrus-associated bacteria. *Annu. Rev. Phytopathol.* **42**, 163–184.

Moreira, L.M., Almeida, N.F., Jr., Potnis, N., Digiampietri, L.A., Adi, S.S., Bortolossi, J.C., da Silva, A.C., da Silva, A.M., de Moraes, F.E., de Oliveira, J.C., de Souza, R.F., Facincani, A.P., Ferraz, A.L., Ferro, M.I., Furlan, L.R., Gimenez, D.F., Jones JB, Kitajima, E.W., Laia, M.L., Leite, R.P. Jr., Nishiyama, M.Y., Rodrigues Neto, J., Nociti, L.A., Norman, D.J., Ostroski, E.H., Pereira, H.A. Jr., Staskawicz, B.J., Tezza, R.I., Ferro, J.A., Vinatzer, B.A. and Setubal, J.C. (2010) Novel insights into the genomic basis of citrus canker based on the genome sequences of two strains of *Xanthomonas fuscans* subsp. *aurantifolii*. *BMC Genomics*, **11**, 238.

Newman, K.L., Almeida, R.P., Purcell, A.H. and Lindow, S.E. (2004) Cell–cell signaling controls *Xylella fastidiosa* interactions with both insects and plants. *Proc. Natl. Acad. Sci. USA*, **101**, 1737–1742.

O'Connell, A., An, S.Q., McCarthy, Y., Schulte, F., Niehaus, K., He, Y.Q., Tang, J.L., Ryan, R.P. and Dow JM. (2013) Proteomics analysis of the regulatory role of Rpf/DSF cell-to-cell signaling system in the virulence of *Xanthomonas campestris*. *Mol. Plant–Microbe Interact.* **26**, 1131–1137.

O'Toole, G.A. and Kolter, R. (1998) Initiation of biofilm formation in *Pseudomonas fluorescens* WCS365 proceeds via multiple, convergent signalling pathways: a genetic analysis. *Mol. Microbiol.* **28**, 449–461.

Petrocelli, S., Tondo, M.L., Daurelio, L.D. and Orellano, E.G. (2012) Modifications of *Xanthomonas axonopodis* pv. *citri* lipopolysaccharide affect the basal response and the virulence process during citrus canker. *PLoS One*, **7**, e40051.

Rigano, L.A., Siciliano, F., Enrique, R., Sendin, L., Filippone, P., Torres, P.S., Qüesta, J., Dow, J.M., Castagnaro, A.P., Vojnov, A.A. and Marano, M.R. (2007) Biofilm formation, epiphytic fitness, and canker development in *Xanthomonas axonopodis* pv. *citri*. *Mol. Plant–Microbe Interact.* **20**, 1222–1230.

Ruhal, R., Kataria, R. and Choudhury, B. (2013) Trends in bacterial trehalose metabolism and significant nodes of metabolic pathway in the direction of trehalose accumulation. *Microb. Biotechnol.* **6**, 493–502.

Saravolac, E.G., Taylor, N.F., Benz, R. and Hancock, R.E. (1991) Purification of glucose-inducible outer membrane protein OprB of *Pseudomonas putida* and reconstitution of glucose-specific pores. *J. Bacteriol.* **173**, 4970–4976.

Schatschneider, S., Huber, C., Neuweger, H., Watt, T.F., Puhler, A., Eisenreich, W., Wittmann, C., Niehaus, K. and Vorhölter, F.J. (2014) Metabolic flux pattern of glucose utilization by *Xanthomonas campestris* pv. campestris: prevalent role of the Entner–Doudoroff pathway and minor fluxes through the pentose phosphate pathway and glycolysis. *Mol. Biosyst.* **10**, 2663–2676.

Sgro, G.G., Ficarra, F.A., Dunger, G., Scarpeci, T.E., Valle, E.M., Cortadi, A., Orellano, E.G., Gottig, N. and Ottado, J. (2012) Contribution of a harpin protein from *Xanthomonas axonopodis* pv. citri to pathogen virulence. *Mol. Plant Pathol.* **13**, 1047–1059.

Shrivastava, R., Basu, B., Godbole, A., Mathew, M.K., Apte, S.K. and Phale, P.S. (2011) Repression of the glucose-inducible outer-membrane protein OprB during utilization of aromatic compounds and organic acids in *Pseudomonas putida* CSV86. *Microbiology*, **157**, 1531–1540.

da Silva, A.C., Ferro, J.A., Reinach, F.C., Farah, C.S., Furlan, L.R., Quaggio, R.B., Monteiro-Vitorello, C.B., Van Sluys, M.A., Almeida, N.F., Alves, L.M., do Amaral, A.M., Bertolini, M.C., Camargo, L.E., Camarotte, G., Cannavan, F., Cardozo, J., Chambergo, F., Ciapina, L.P., Cicarelli, R.M., Coutinho, L.L., Cursino-Santos, J.R., El-Dorry, H., Faria, J.B., Ferreira, A.J., Ferreira, R.C., Ferro, M.I., Formighieri, E.F., Franco, M.C., Greggio, C.C., Gruber, A., Katsuyama, A.M., Kishi, L.T., Leite, R.P., Lemos, E.G., Lemos, M.V., Locali, E.C., Machado, M.A., Madeira, A.M., Martinez-Rossi, N.M., Martins, E.C., Meidanis, J., Menck, C.F., Miyaki, C.Y., Moon, D.H., Moreira, L.M., Novo, M.T., Okura, V.K., Oliveira, M.C., Oliveira, V.R., Pereira, H.A., Rossi, A., Sena, J.A., Silva, C., de Souza, R.F., Spinola, L.A., Takita, M.A., Tamura, R.E., Teixeira, E.C., Tezza, R.I., Trindade dos Santos, M., Truffi, D., Tsai, S.M., White, F.F., Setubal, J.C. and Kitajima, J.P. (2002) Comparison of the genomes of two Xanthomonas pathogens with differing host specificities. *Nature*, **417**, 459–463.

Slater, H., Alvarez-Morales, A., Barber, C.E., Daniels, M.J. and Dow, J.M. (2000) A two-component system involving an HD-GYP domain protein links cell–cell signalling to pathogenicity gene expression in *Xanthomonas campestris*. *Mol. Microbiol.* **38**, 986–1003.

Stankowski, J.D., Mueller, B.E. and Zeller, S.G. (1993) Location of a second O-acetyl group in xanthan gum by the reductive-cleavage method. *Carbohydr. Res.* **241**, 321–326.

Sutherland, I.W. (1998) Novel and established applications of microbial polysaccharides. *Trends Biotechnol.* **16**, 41–46.

Tang, J.L., Liu, Y.N., Barber, C.E., Dow, J.M., Wootton, J.C. and Daniels, M.J. (1991) Genetic and molecular analysis of a cluster of rpf genes involved in positive regulation of synthesis of extracellular enzymes and polysaccharide in *Xanthomonas campestris* pathovar campestris. *Mol. Gen. Genet.* **226**, 409–417.

Wei, C.L., Lin, N.T., Weng, S.F. and Tseng, Y.H. (1996) The gene encoding UDP-glucose pyrophosphorylase is required for the synthesis of xanthan gum in *Xanthomonas campestris*. *Biochem. Biophys. Res. Commun.* **226**, 607–612.

Wilson, W.A., Roach, P.J., Montero, M., Baroja-Fernandez, E., Munoz, F.J., Eydallin, G., Viale, A.M. and Pozueta-Romero, J. (2010) Regulation of glycogen metabolism in yeast and bacteria. *FEMS Microbiol. Rev.* **34**, 952–985.

Wylie, J.L. and Worobec, E.A. (1995) The OprB porin plays a central role in carbohydrate uptake in *Pseudomonas aeruginosa*. *J. Bacteriol.* **177**, 3021–3026.

Yan, Q. and Wang, N. (2011) The ColR/ColS two-component system plays multiple roles in the pathogenicity of the citrus canker pathogen *Xanthomonas citri* subsp. *citri*. *J. Bacteriol.* **193**, 1590–1599.

Yan, Q., Hu, X. and Wang, N. (2012) The novel virulence-related gene nlxA in the lipopolysaccharide cluster of *Xanthomonas citri* ssp. *citri* is involved in the production of lipopolysaccharide and extracellular polysaccharide, motility, biofilm formation and stress resistance. *Mol. Plant Pathol.* **13**, 923–934.

Yu, N.Y., Wagner, J.R., Laird, M.R., Melli, G., Rey, S., Lo, R., Dao, P., Sahinalp, S.C., Ester, M., Foster, L.J. and Brinkman, F.S. (2010) PSORTb 3.0: improved protein subcellular localization prediction with refined localization subcategories and predictive capabilities for all prokaryotes. *Bioinformatics*, **26**, 1608–1615.

Zimaro, T., Thomas, L., Marondedze, C., Garavaglia, B.S., Gehring, C., Ottado, J. and Gottig, N. (2013) Insights into *Xanthomonas axonopodis* pv. *citri* biofilm through proteomics. *BMC Microbiol.* **13**, 186.

Zimaro, T., Thomas, L., Marondedze, C., Sgro, G.G., Garofalo, C.G., Ficarra, F.A., Gehring, C., Ottado, J. and Gottig, N. (2014) The type III protein secretion system contributes to *Xanthomonas citri* subsp. *citri* biofilm formation. *BMC Microbiol.* **14**, 96.

SUPPORTING INFORMATION

Additional Supporting Information may be found in the online version of this article at the publisher's website:

Fig. S1 Representative scheme of the biosynthesis of xanthan. The components of the lipid-linked intermediates are

represented as follows: Glc, glucose; Man, mannose; GlcA, glucuronic acid; Ac, acetyl group; Pyr, pyruvyl group. (Adapted from Katzen *et al.*, 1999.)

Fig. S2 Analysis of *Xanthomonas citri* ssp. *citri* (Xcc), XccΔoprB and XccΔoprBc growth in different media. Growth curves of Xcc, XccΔoprB and XccΔoprBc in Nutrient Broth (NB) (A), Silva–Buddenhagen (SB) (B) and XVM2 (C) media. At the times stated, bacteria were diluted and plated, and the number of colony-forming units (cfu)/mL was calculated. Each point represents the mean of three independent experiments. Error bars are standard deviations. The data were statistically analysed using one-way analysis of variance (ANOVA) ($P < 0.05$).

Fig. S3 Relative expression of *gumD* in *Xanthomonas citri* ssp. *citri* (Xcc), XccΔoprB and XccΔoprBc. Reverse transcription-quantitative polymerase chain reaction (RT-qPCR) assay to determine *gumD* expression of the different strains relative to Xcc. Total RNA was extracted and cDNA was synthesized using M-MLV reverse transcriptase (RT) (Promega, Fitchburg, Wisconsin, USA) and the oligonucleotide dN6. The oligonucleotides used to analyse the expression of *gumD* have been described elsewhere (Zimaro *et al.*, 2014) and, as a reference gene, a fragment of 16S was amplified in the same reaction conditions. The values are the mean of three independent experiments. The results were analysed using one-way analysis of variance (ANOVA) ($P < 0.05$).